1521-0111/12/8102-228–238$25.00
MOLECULAR PHARMACOLOGY
Copyright © 2012 The American Society for Pharmacology and Experimental Therapeutics
Mol Pharmacol 81:228–238, 2012

Vol. 81, No. 2
72967/3743511

Cancer-Preventive Rexinoid Modulates Neutral Lipid Contents of Mammary Epithelial Cells through a Peroxisome Proliferator-Activated Receptor γ-Dependent Mechanism

Iván P. Uray, Jennifer M. Rodenberg, Reid P. Bissonnette, Powel H. Brown, and Michael A. Mancini

Department of Molecular and Cellular Biology, Baylor College of Medicine, Houston, Texas (I.P.U., P.H.B., M.A.M.); Department of Clinical Cancer Prevention, The University of Texas M.D. Anderson Cancer Center, Houston, Texas (I.P.U., J.M.R., P.H.B.); and Ligand Pharmaceuticals, San Diego, California (R.P.B.)

Received April 17, 2011; accepted October 28, 2011

ABSTRACT

Synthetic rexinoids effectively suppress both estrogen receptor-positive and estrogen receptor-negative mammary tumors in animal models, which makes them prime candidates for a novel class of cancer-preventive agents. When used in combination with chemotherapy for non–small-cell lung cancer, the rexinoid bexarotene was most effective for patients who developed hypertriglyceridemia as a side effect. Although serum triglycerides originate from the liver, the effect of bexarotene on lipogenesis in breast epithelial cells is not known. Gene expression studies with normal mammary epithelial cells indicated that rexinoids modulate lipid metabolism, particularly enzymes involved in triglyceride synthesis. High-content analysis revealed dose-dependent accumulation of neutral lipids within adipocyte differentiation-related protein-associated cytoplasmic lipid droplets after long-term bexarotene treatment. Bexarotene also induced mRNA and protein levels for peroxisome proliferator-activated receptor (PPAR) γ, whereas selective knockdown of PPARγ attenuated the induction of both lipid droplets and adipocyte differentiation-related protein. Pharmacological activation of PPARγ, but not PPARα or retinoic acid receptors, effectively induced lipid accumulation. Furthermore, the combination of the PPARγ agonist rosiglitazone with bexarotene synergistically suppressed the growth of human mammary epithelial cells and revealed a strong, nonlinear, inverse correlation of cell growth with lipid droplet accumulation in the cell population. These findings indicate that rexinoids activate a lipogenic program in mammary epithelial cells through a retinoid X receptor/PPARγ-mediated mechanism. It is noteworthy that combining low doses of bexarotene with the PPARγ agonist rosiglitazone provides effective growth suppression of mammary epithelial cells, potentially dissociating systemic adverse effects associated with standard bexarotene treatment from the antiproliferative effects on mammary epithelium.

Introduction

The feasibility of chemoprevention of estrogen receptor (ER)-positive breast cancers has been established with the use of selective estrogen response modifiers (Cuzick et al., 2003) and the demonstration that ligand-dependent transcription factors are ideal targets for cancer-preventive agents (Uray and Brown, 2006). However, effective preventive agents for ER-negative breast cancers still need to be developed (Uray and Brown, 2011). Retinoids that selectively activate retinoid X receptors (RXRs) (rexinoids) efficiently suppress the development of mammary tumors in animal breast cancer models (Gottardis et al., 1996), alone or in combination with agents with different mechanisms of action. Unlike antiestrogenic compounds, rexinoids prevent the development of both ER-positive and ER-negative breast tumors (Bischoff et al., 1999; Wu et al., 2002). Bexarotene is a synthetic rexinoid that has been approved for the treatment of refractory, cutaneous, T-cell lymphomas and has been tested against other cancer types in combination with various chemotherapeutic protocols, with moderate success. Although the cancer-preventive potential of bexarotene exceeds

This work was supported by the National Institutes of Health National Cancer Institute [Grant R03-CA137777] (to I.P.U. and M.A.M.), [Grant R01-CA78480] (to P.H.B.); and in part by seed funding from the Hankamer Foundation (to M.A.M.).

Article, publication date, and citation information can be found at http://molpharm.aspetjournals.org.

http://dx.doi.org/10.1124/mol.111.072967.

ABBREVIATIONS: HMEC, human mammary epithelial cell; PPAR, peroxisome proliferator-activated receptor; RXR, retinoid X receptor; ER, estrogen receptor; DAPI, 4′,6-diamidino-2-phenylindole; siRNA, small interfering RNA; SCD1, stearoyl-CoA desaturase 1; ACSL1, acyl-CoA synthetase 1; DGAT1, diacylglycerol acyl-transferase 1; ADFP, adipocyte differentiation-related protein; LXR, liver X receptor; RT, reverse transcription; NA, numerical aperture; PCR, polymerase chain reaction.

its effectiveness in the treatment of existing cancers, its clinical use is affected by dose-limiting side effects, primarily hypertriglyceridemia arising from elevated hepatic very low density lipoprotein production (de Vries-van der Weij et al., 2009). It is noteworthy that a phase III clinical trial comparing the effects of chemotherapy and chemotherapy plus bexarotene for patients with advanced non–small-cell lung cancer found that the occurrence of high-grade hypertriglyceridemia was correlated with increased survival rates for bexarotene-treated patients (Blumenschein et al., 2008), which suggests a connection between lipid metabolism and cell growth control. Conversely, although it induced tumor regression in several rodent mammary carcinoma models, its antitumor effects were correlated with the induction of adipocyte-specific gene expression (Agarwal et al., 2000). In contrast to the causes for elevated systemic triglyceride levels, the consequences of rexinoid treatment for the lipid metabolism of epithelial cells, the actual targets of cancer prevention, are not well characterized. Our previous studies indicated that bexarotene regulates the expression of genes involved in lipid metabolism (Kim et al., 2006; Abba et al., 2008). Differentiation and lactation in the mammary gland also are associated with lipid accumulation and expression of perilipins, highly phosphorylated adipocyte proteins that are localized at the surface of lipid droplets, in secretory cells as a result of a concerted, developmentally regulated program to increase the availability of fatty acids necessary for lipid synthesis (Russell et al., 2007). Therefore, we adopted a high-throughput, image-based assay (e.g., high-content analysis) to evaluate quantitatively the effects of rexinoids on lipid metabolism, proliferation, and nuclear receptor levels in mammary epithelial cells. An additional goal of this study was to elucidate whether the systemic side effects of bexarotene could be dissociated from its growth-suppressive effect on the mammary epithelium.

The cancer-preventive effects of rexinoids are largely attributed to their abilities to elicit cell-cycle arrest and to inhibit mammary epithelial cell growth both in vitro and in vivo (Wu et al., 2006; Li et al., 2007). Therefore, proliferation markers currently serve as surrogate biomarkers of a cancer-preventive effect in the breast. Bexarotene-induced hypertriglyceridemia is controlled through dose adjustment of the drug or the addition of lipid-lowering therapy (Assaf et al., 2006); however, it remains to be shown whether the treatment retains its chemopreventive effect at reduced dosages.

Our data show that the RXR-selective retinoid bexarotene induces the accumulation of neutral lipid-containing cytoplasmic droplets by activating an RXR/PPARγ-dependent lipogenic program in mammary epithelial cells. This increase in neutral lipid content is concomitant with the up-regulation of PPARγ levels as well as the enzymes required for triglyceride synthesis. The data also demonstrate that the combination of low-dose bexarotene with the PPARγ agonist rosiglitazone acts synergistically to suppress the growth of mammary epithelial cells. Because marked lipid accumulation occurs at higher bexarotene doses, potentially adverse responses may be dissociated from the antiproliferative effects of bexarotene when combined with rosiglitazone.

Materials and Methods

Cell Culture. Normal human mammary epithelial cells (HMECs), derived from healthy women who had undergone reduction mammoplasties, were purchased from Clonetics Corp. (San Diego, CA). Cells from at least five different isolates were used in the experiments, with their passage numbers kept below 12. HMECs were maintained in mammary epithelial basal medium supplemented with 50 μg/ml bovine pituitary extract, 5 μg/ml insulin, 10 ng/ml human recombinant epidermal growth factor, 0.5 μg/ml hydrocortisone, 30 μg/ml gentamicin, and 15 ng/ml amphotericin-B (Clonetics Corp.). Cells were cultured in a humidified environment at 37°C with 5% CO_2 in air.

Ligands. The synthetic RXR ligands bexarotene (Targretin, LGD1069) and LGD100268 were a kind gift from Dr. Reid Bissonnette at Ligand Pharmaceuticals (San Diego, CA). Rexinoids were dissolved and kept in 50:50 dimethylsulfoxide/ethanol solvent and were used at a final concentration of 1 μM, unless otherwise indicated. siRNA duplexes were designed and synthesized with Sigma-Proligo (Sigma-Aldrich, St. Louis, MO), and Dharmafect 1 siRNA transfection reagent was purchased from Thermo-Fisher Scientific (Waltham, MA).

Fluorescence Microscopy. For general fluorescent imaging purposes, HMECs were seeded on 0.17-mm glass coverslips 24 h before treatment. For high-throughput, high-content applications, HMECs were plated on Greiner Bio-One (Longwood, FL) 96-well or Aurora (NEXUS Biosystems, Poway, CA) 384-well optical plastic-bottomed test plates at densities of 2000 or 500 cells per well, respectively. Cells were then exposed to bexarotene, solvent, or other nuclear receptor ligands for 24 h. Compound dilution and addition to multiwell plates were performed by using a Beckman Coulter (Fullerton, CA) NX liquid handling system. After completion of the treatment, plates were washed with ice-cold phosphate-buffered saline and fixed for 20 min at room temperature with 4% formaldehyde. After fixation, cells were briefly permeabilized (2 min) with 0.1% Triton X-100 and were prepared for imaging through washing in phosphate-buffered saline and addition of a 1 μg/ml DAPI solution. For the specific detection of triglycerides as dominant neutral lipids within rexinoid-treated cells, we used the green fluorescent dye LipidTox (Invitrogen, Carlsbad, CA) at 1:500 neutral lipid stain. For the immunofluorescent detection of proteins, cells were incubated for 30 min with 5% nonfat milk in Tris-buffered saline, followed by incubation overnight at 4°C with antibodies against PPARγ (1:200), RXRα (1:500), or adipocyte differentiation-related protein (ADFP) (1:200). Fluorescent images were captured by using an IC 100 automated cytometer (Beckman Coulter) with CytoShop 2.0 (Beckman Coulter) or by using an ImageXpress Micro high-throughput imager (Molecular Devices, Sunnyvale, CA). Three 8-bit images per field were acquired with a Nikon (Melville, NY) S Fluor 20×/0.75 NA or S Fluor 40×/0.90 NA objective and 2 × 2 binning (DAPI, green fluorescent protein/Alexa Fluor 488, or Alexa Fluor 594), which resulted in 0.344 × 0.344 μm^2/pixel grayscale bitmapped images. The fluorophores used (i.e., DAPI, LipidTox, and Alexa Fluor 594) were excited at 358, 488, and 594 nm, respectively, by using appropriate bandpass filters. In general, 12 to 64 fields (with a minimum of 200 cells) per well were imaged for analysis. Apoptotic and fragmented cells, as well as nonsegmentable structures, were excluded from analysis. High-resolution, three-dimensional images were acquired and deconvolved with a DeltaVision Core fluorescent image restoration system with a 40×/0.95 NA "dry" objective or a 60×/1.3 NA oil objective (Applied Precision Instruments, Issaquah, WA).

Image Analysis and Quantitation. Commercially available image analysis algorithms developed specifically to identify and to quantitate subcellular structures accurately were used to create overlay masks, which allowed measurement of lipid droplets and nuclear structures and colocalization of lipid-associated proteins. Analyses of microscopy data were performed with the lipid droplet and colocalization algorithms of CyteSeer image analysis software

(Vala Sciences, San Diego, CA), as described in detail previously (McDonough et al., 2009). In brief, after segmentation of cell nuclei by using the DAPI channel, pixels identified as being above the threshold in the lipid or antibody image with each algorithm were defined as representing the lipid mask or the protein mask, respectively. The lipid content of a cell was measured as the total integrated intensity of the lipid signal (in the fluorescein isothiocyanate channel) under the lipid mask (e.g., segmented lipid droplets) (see Fig. 2). Lipid droplet-derived measurements and all other (>60) measurements from the areas of each mask were reported on a per-cell basis. The resulting numerical data included both single-cell and well-by-well measurements, representing data averaged across all cells imaged within each well. Cells whose nuclei crossed the edge of an image were excluded from measurements. Furthermore, as a measure of health/toxicity, cells with nuclear DNA contents <50% of the average value corresponding to G_0/G_1 were excluded from further analysis. To assess quantitatively the suitability of the assay for subsequent use in high-content screening experiments, we determined *Z*-factor (*Z′*) values for the various measurements available through the image analysis algorithms. The *Z′* statistic is commonly used to quantify the robustness of assays (Zhang et al., 1998), $Z' = 1 - 3(SD_{max} + SD_{min})/(X_{max} - X_{min})$, where SD is the S.D. and *X* is the mean. For *Z′* to be positive (e.g., $Z' > 0$), the sum of the S.D. values from the maximal and minimal measurements must be less than one third of the range of the assay (X_{max} to X_{min}). For an ideal assay in which there is no variation in the determinations (i.e., S.D. = 0), *Z′* equals 1. *Z′* values above 0.2 are considered "screenable," and *Z′* values above 0.5 are considered excellent. The *Z′* values for the measurements of both cell counts and total cellular lipid signal intensities under the lipid mask exceeded 0.55, which indicated a very low chance of false-positive results arising from random variation in a high-throughput screening application.

RNA Extraction and Measurement of Transcript Levels. Total RNA was extracted by using an RNeasy kit (QIAGEN, Valencia, CA), according to the manufacturer's instructions. Reverse transcription (RT) was performed in triplicate, with a non-RT control sample lacking reverse transcriptase assayed in parallel, to control for amplification attributable to genomic DNA contamination. Gene-specific primers and dual-labeled TaqMan probes (Applied Biosystems, Foster City, CA) used in quantitative RT-polymerase chain reaction (PCR) assays to measure mRNA levels for lipogenic genes are listed in Table 1. Transcript quantitation based on real-time monitoring of amplification was performed by using an ABI Prism 7900 HT sequence detection system (Applied Biosystems), with 40 cycles of 95°C for 12 s and 60°C for 30 s. Values for transcripts in unknown samples were obtained through interpolation of their threshold cycle values (PCR cycles to threshold) on a standard curve derived with known amounts of cognate, amplicon-specific, synthetic oligonucleotides. Transcript levels were normalized with respect to the level of cyclophilin mRNA.

Western Blot Analysis. Proteins extracts were solubilized, fractionated through 10% SDS-polyacrylamide gel electrophoresis, and transferred to a polyvinylidene fluoride membrane. After blocking with 5% bovine serum albumin, the membrane was probed with antibodies against stearoyl-CoA desaturase 1 (SCD1) (1:200, sc14715; Santa Cruz Biotechnology, Santa Cruz, CA), acyl-CoA synthetase 1 (ACSL1) (1:1000, 4047; Cell Signaling Technology, Danvers, MA), or diacylglycerol acyl-transferase 1 (DGAT1) (1:200, SAB2500307; Sigma-Aldrich) and subsequently incubated with peroxidase-conjugated secondary antibody (1:5000; GE Healthcare, Chalfont St. Giles, Buckinghamshire, UK). Signals were observed through enhanced chemiluminescence detection (Thermo Fisher Scientific). After stripping (30 min at 50°C with 2% SDS and 100 mM β-mercaptoethanol), the same membrane was reprobed with anti-β-actin antibody (1:5000; Sigma-Aldrich Co.). Densitomeric quantitation was performed by using ImageJ (http://rsbweb.nih.gov/ij/). The protein levels of lipogenic enzymes were normalized with respect to β-actin.

Selective Gene Knockdown Experiments. To assess the effects of gene silencing on target gene expression and lipid accumulation, 10^4 cells were seeded on 24-well, tissue-culture plates 24 h before transfection. Transfection conditions were optimized for the highest level of knockdown at the lowest toxicity, by using pools of three gene-specific siRNAs at 10 nM concentrations and Dharmafect 1 transfection reagent (Dharmacon, Lafayette, CO). Suppression of transcript levels exceeding 70%, as measured through real-time quantitative RT-PCR, was considered acceptable.

Statistical Analysis. Statistical significance was determined by using Student's *t* test or two-tailed analysis of variance. A *p* value of <0.05 was considered statistically significant. Values are presented as mean ± S.D. values. Synergy between two agents was assessed quantitatively by constructing isobolograms with CalcuSyn software (Biosoft, Cambridge, UK), which performs drug dose-effect calculations by using the median effect method described by Chou and Talalay (1984). Distinction from additivity and statistical significance of the synergistic effect were established through direct comparisons of the combination with the relative effects of the two individual drugs at their respective ED_{50} values, as described by Laska et al. (1994). Comparisons between groups were performed with two-way Student's *t* tests.

Results

It is now well established that rexinoids induce changes in the cell cycle and suppress the growth of nontransformed mammary epithelial cells (HMECs) through the modulation of growth-regulatory transcription factors and signaling molecules (Wu et al., 2006; Uray et al., 2009). However, the growth-suppressive effects of these agents do not strictly correlate with their chemopreventive potential, which suggests that other factors also contribute to the cancer-preventive activity of rexinoids. In addition to regulating cell growth, our previous studies indicated that the synthetic rexinoid bexarotene (LGD1069, Targretin) preferentially regulates the expression of genes involved in lipid metabolism (Kim et al., 2006; Abba et al., 2008). Quantitative RT-PCR

TABLE 1

Primer and probe sequences used in quantitative real-time RT-PCR assays to measure mRNA levels of lipogenic genes

Transcript quantitation based on real-time monitoring of amplification was carried out according to the parameters defined under *Materials and Methods*.

Gene Name or Symbol	GenBank Accession No.	Primers (5′→3′)		TaqMan Probe (5′→3′)
		Forward	Reverse	
SCD1	NM_005063	CACCTCTTCGGATATCGTCCT	GTAGTTGTGGAAGCCCTCACC	FAM-ATGACAAGAACATTAGCCCCCGGGAG-BHQ
ACSL1	NM_001995	AGATCTTGCAGTAATTTGTTTCACAA	CGCTCACTATGTTTCGGTGAGT	FAM-TGGAACTACAGGCAACCCCAAAGGAG-BHQ
DGAT1	NM_012079	TGGAACATCCCTGTGCACA	TGCCCCGTCGAAGCAT	FAM-TGGTGCATCAGACACTTCTACAAGCCC-BHQ
Adfp	NM_001122	GTGACTGGCAGTGTGGAGAAG	TCCGACTCCCCAAGACTGT	FAM-CCAAGTCTGTGGTCAGTGGCAGCA-BHQ
PPARγ	NM_138712	ATGCTGGCCTCCTTGATGA	GCTTTCGCAGGCTCTTTAGAA	FAM-TCTCATATCCGAGGGCCAAGGCTTC-BHQ
Cyclophilin	NM_021130	ACGGCGAGCCCTTGG	TTTCTGCTGTCTTTGGGACCT	FAM-CGCGTCTCCTTTGAGCTGTTTGCA-BHQ

FAM, 5-carboxyfluorescein; BHQ, black hole quencher.

analysis of mRNA levels showed that the expression of key enzymes involved in triglyceride synthesis, such as ACSL1, SCD1, and DGAT1, were significantly up-regulated after 24 h of bexarotene treatment (Fig. 1A). To detect changes in the protein levels of these lipogenic enzymes, we performed Western-blot analyses by using total cell extracts from HMECs treated for 48 h with solvent or 1 μM bexarotene (Fig. 1B). Densitometric analysis revealed that all three of these enzymes, ACSL1, SCD1, and DGAT1, were induced by bexarotene, 5-fold ($p < 0.005$), 2.3-fold ($p < 0.05$), and 1.75-fold ($p < 0.005$), respectively (Fig. 1C). Furthermore, when we examined the lipid content of HMECs after long-term treatment with 1 μM bexarotene by using the general lipid dye Oil Red O, qualitative analysis through bright-field imaging indicated an overall increase in cytoplasmic lipid contents after a period of no less than 4 days of bexarotene treatment (data not shown).

To discriminate and to quantify cellular phenotypic changes in response to rexinoids on a cell-by-cell basis, we developed a high-content image-based assay that simultaneously measured cytoplasmic lipid features (e.g., lipid droplet number and size), nuclear DNA content, expression of lipid-

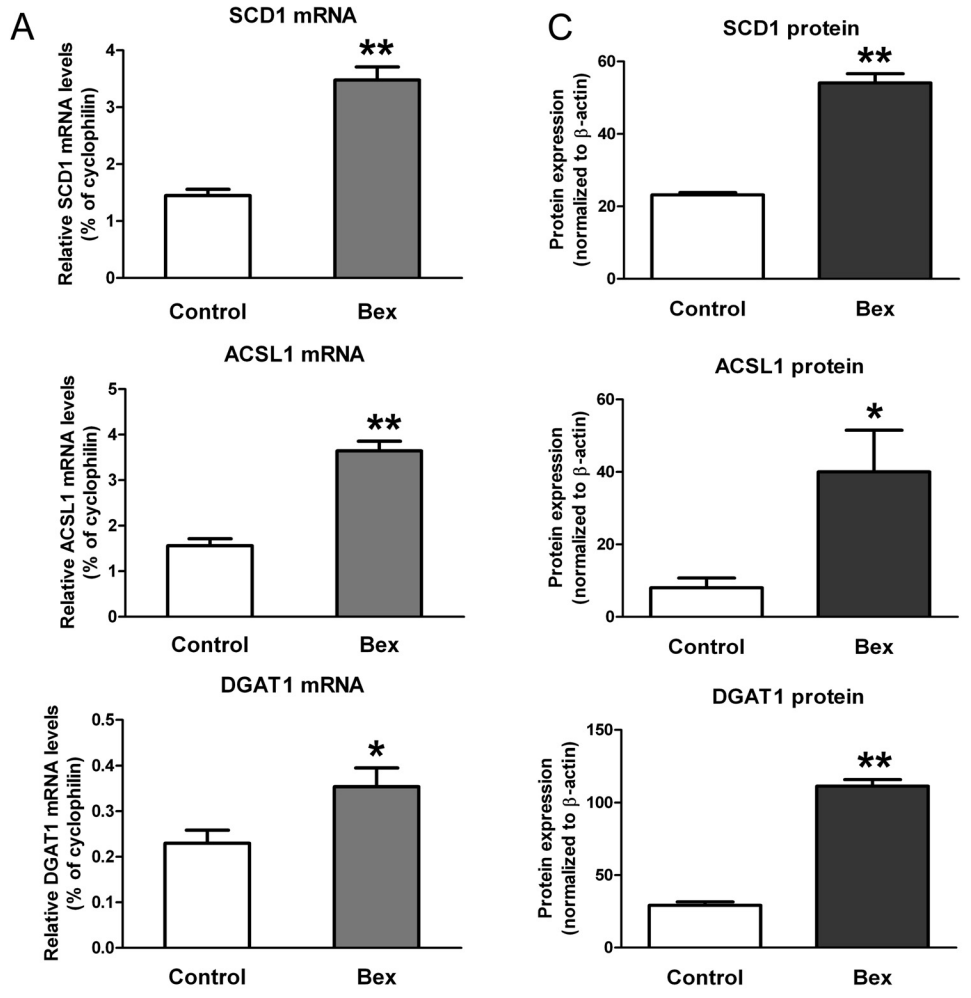

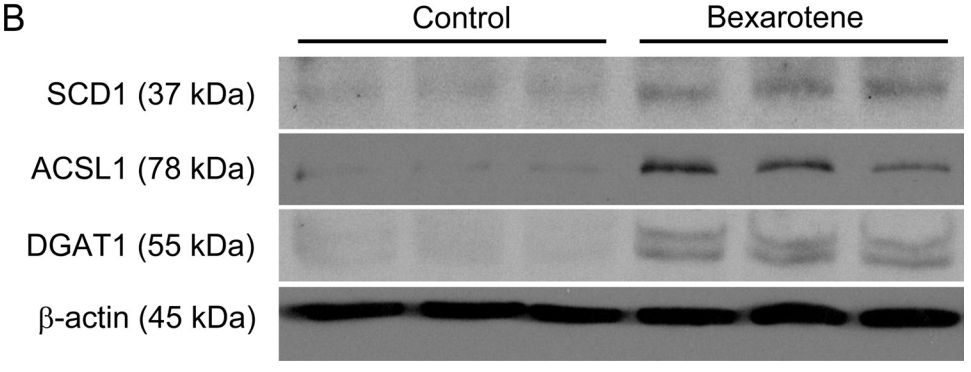

Fig. 1. Quantitation of mRNA and protein levels for enzymes required for triglyceride synthesis in normal mammary epithelial cells. A, HMECs were cultured at low confluence and were treated with solvent or 1 μM bexarotene (Bex) for 24 h. Subsequently, RNA was extracted and quantitative real-time RT-PCR was used to determine the expression levels of SCD1, ACSL1, and DGAT1. Molecule numbers were extrapolated from a standard curve, and relative mRNA levels were expressed with respect to levels of the housekeeping gene cyclophilin. **, $p < 0.005$; *, $p < 0.05$. B, Western-blot analysis of SCD1, ACSL1, and DGAT1 protein levels in cell extracts from HMECs treated with vehicle or 1 μM bexarotene for 48 h. C, densitometric analysis of the Western blots for quantitation of protein expression of the lipogenic enzymes SCD1, ACSL1, and DGAT1. **, $p < 0.005$; *, $p < 0.05$.

associated proteins, and transcription factors that regulate lipid metabolism. High-resolution deconvolution microscopy and three-dimensional viewing confirmed the presence of elevated levels of neutral lipids and indicated the formation of small adipocyte-like lipid droplets in the cytoplasm of HMECs treated with bexarotene (Fig. 2, A and B). Quanti-

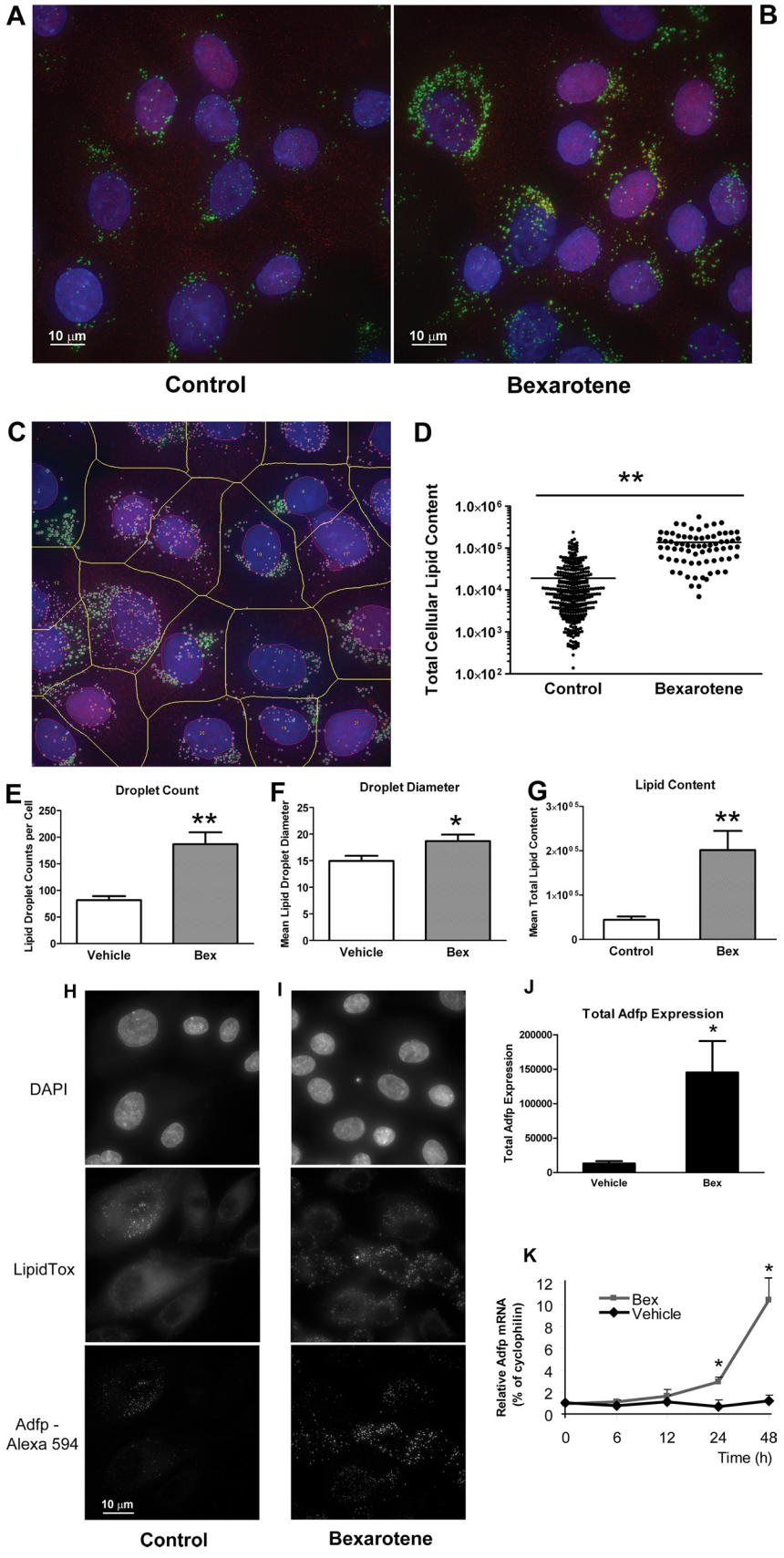

Fig. 2. Multiparametric assessment of lipid accumulation and expression and localization of RXRα and ADFP in HMECs in the absence or presence of bexarotene. A and B, cells were treated with vehicle or 1 μM bexarotene for 96 h, fixed, and stained for RXRα (Alexa594; red), neutral lipids (LipidTox; green), and DNA (DAPI; blue). Twenty *Z*-stack images per treatment, taken at 60× magnification with a DeltaVision system (Applied Precision Instruments), were deconvolved and maximum-projected into single, plain, red/green/blue images for analysis. Scale bars, 10 μm. C, analysis of the labeled cellular compartments through segmentation of the nuclei, lipid droplets, and RXRα protein with CyteSeer software (Vala Sciences, San Diego, CA) (McDonough et al., 2009). D, cell-by-cell measurement of the neutral lipid contents in lipid droplets after bexarotene treatment. E–G, lipid droplet metrics in HMECs. Lipid droplet counts formed as a result of the accumulation of neutral lipids (E), average lipid droplet diameter (F), and average neutral lipid content (G) were quantitated in HMECs after 4 days of bexarotene (Bex) treatment. H and I, immunofluorescent labeling of ADFP (Alexa594; red channel) localized to the outer rims of lipid droplets (labeled with LipidTox; green channel) in bexarotene-treated cells. Nuclear DNA was stained with DAPI. Scale bars, 10 μm. J, quantitation of ADFP protein on the basis of cellular integrated signal intensity from deconvolved projected images at 60× magnification. K, progression of ADFP mRNA levels in the absence (Vehicle) or presence (Bex) of 1 μM bexarotene. **, $p < 0.005$; *, $p < 0.05$.

tative assessment of the rexinoid response on the basis of changes in the cellular phenotype was achieved through specific segmentation of lipid droplets, cell nuclei, and cell boundaries and quantitation of RXRα immunolabeling (Fig. 2C). Cell-by-cell analysis after automated high-throughput microscopy revealed that, in more than 90% of the cells, the neutral lipid content exceeded the average for untreated cells after bexarotene treatment and overall was 7-fold higher (Fig. 2D). These data indicated a robust lipid content increase (albeit heterogeneous among individual cells). It is noteworthy that we observed similar levels of neutral lipid accumulation in five different batches of primary mammary epithelial cells, derived from different individuals.

The image data further demonstrated that the increase in intracellular lipid droplet counts (Fig. 2E) was associated with small but statistically significant increases in both droplet diameter (Fig. 2F) and surface area (data not shown). The product of the changes in these parameters and the increased lipid droplet counts amounted to a marked increase in total cellular neutral lipid content (Fig. 2G) with bexarotene treatment. Lipid droplet counts were highly correlated with the total intensity of the lipid signal ($r^2 = 0.78$, $p < 0.0001$; data not shown). Furthermore, by using deconvolution-based three-dimensional imaging, we verified that quantitation of both integrated pixel intensities and lipid droplet counts provided good estimates of the accumulated lipid mass.

By using a three-compartment masking approach [e.g., nuclei with DAPI, lipid droplets with LipidTox, and cell boundaries with CellMask (Invitrogen), a general protein dye], fluorescently labeled cytoplasmic lipid droplets were shown to localize predominantly with immunolabeled ADFP (adipophilin), a protein known to play a role in adipogenic differentiation (Russell et al., 2007). Furthermore, total and lipid droplet-associated ADFP levels were markedly increased in bexarotene-treated cells (Fig. 2, H–J). Bexarotene also exponentially induced ADFP mRNA levels 48 h after drug treatment (Fig. 2K). In summary, elevated triglyceride production seems to result primarily in an increase in the number of lipid droplets, rather than a marked increase in their size.

To assess the sensitivity of HMECs to bexarotene, cells were treated with escalating doses of the drug over a period of 4 days (Fig. 3A). Lipid accumulation occurred in a dose-dependent manner, and a significant increase could be defined with bexarotene levels below 0.1 μM, a concentration lower than that needed to suppress growth significantly in these cells. Immunofluorescent labeling of RXRα indicated its ubiquitous expression, and RXRα levels in the nuclei at the time of imaging were unaffected by bexarotene doses up to 1 μM (data not shown). The ratio between nuclear and cytoplasmic fractions of RXRα was determined from the integrated pixel intensities under the nuclear versus cytoplasmic masks. As expected, the majority of RXRα was always in the nuclear fraction, although some cytoplasmic labeling was also detected consistently. However, neither the number of lipid droplets nor the amount of cytoplasmic lipids showed any correlation with RXR expression.

Rexinoids can activate a number of RXR-containing permissive heterodimers to regulate the expression of target genes of their partners. Therefore, we compared the effects of agonists of PPARs and retinoid receptors on lipid accumulation in HMECs. Rosiglitazone is an insulin-sensitizer thiazolidinedione that is used clinically for the treatment of type 2 diabetes mellitus and activates PPARγ selectively (Kahn and McGraw, 2010). We found that both the RXR agonists bexarotene and LGD100268 and the PPARγ agonist rosiglitazone increased the number of lipid droplets in primary HMECs, whereas a PPARα agonist (WY14643) and a pan-RAR agonist [(*E*)-4-[2-(5,6,7,8-tetrahydro-5,5,8,8-tetramethyl-2-naphthalenyl-1-propenyl]benzoic acid (TTNPB)] were ineffective (Fig. 3B). Furthermore, immunofluorescent quantitation of PPARγ expression after bexarotene treatment showed that both nuclear PPARγ protein and mRNA levels increased (Fig. 3, C and D, left). Next, siRNA transfections were performed to verify that PPARγ was required for both lipid accumulation and droplet formation. Knockdown of PPARγ in HMECs markedly reduced the mRNA levels for PPARγ, compared with those observed for the control (siNT) (Fig. 3D, right). Transfections of siRNAs against PPARα, PPARδ, or RXRα resulted in more than 80% reductions in the respective target mRNA levels but had no impact on PPARγ expression, as measured with quantitative RT-PCR (data not shown). Figure 3E shows the comparison of the neutral lipid contents of HMECs treated with vehicle or bexarotene after siRNA-mediated knockdown of RXRα, PPARα, PPARδ, and PPARγ. Bexarotene induced significant induction of lipid contents in all knockdown groups; however, the extents of the changes were markedly different, depending on the selective suppression of receptors. Statistical tests (analysis of variance and Dunnett's multiple-comparison post hoc test) comparing the changes in lipid contents revealed that the bexarotene-induced changes in lipid contents in the control knockdown group (siNT) were significantly ($p < 0.05$) different from those in groups transfected with siRNAs against RXRα, PPARδ, or PPARγ but not PPARα (Fig. 3E), which indicated that suppression of RXRα and PPARγ decreased the ability of bexarotene to induce lipid accumulation. In addition, silencing of PPARγ abrogated the induction of ADFP mRNA (Fig. 3F).

Individual ligand experiments were then followed by combined treatments with rosiglitazone and bexarotene. As shown in Fig. 4A, bexarotene (1 μM) and rosiglitazone (2 μM) in combination were more than twice as effective as either drug alone. The statistical analysis indicated a significant difference in cellular lipid contents of control and bexarotene-treated cells, as well as control and bexarotene- plus rosiglitazone-treated cells. In comparison, the extent of change with bexarotene alone was significantly different from the change induced by the combination of bexarotene plus rosiglitazone. In contrast, the cellular neutral lipid content was inversely proportional to cell counts at the end of the 6-day treatment (Fig. 4B). Although rosiglitazone was only moderately growth-suppressive by itself, it enhanced the growth suppression elicited by bexarotene. To determine whether the effects of the two ligands were additive or synergistic, we performed combined dose-response experiments with a matrix of various dose combinations, including combinations involving nanomolar concentrations. Cell proliferation was determined through image-based cell counting (triplicate wells, with 45 imaged microscopic fields per well) after 4 days of treatment (Fig. 5A). The cell proliferation dose-response curve for HMECs with bexarotene alone indicated an EC_{50} of 0.1 μM; rosiglitazone alone showed an EC_{50} of 3.1 μM. The isobologram resulting from the combinations of incremental doses of these two agents indicated that one or both constituents contributed to the growth-suppressive effect to a

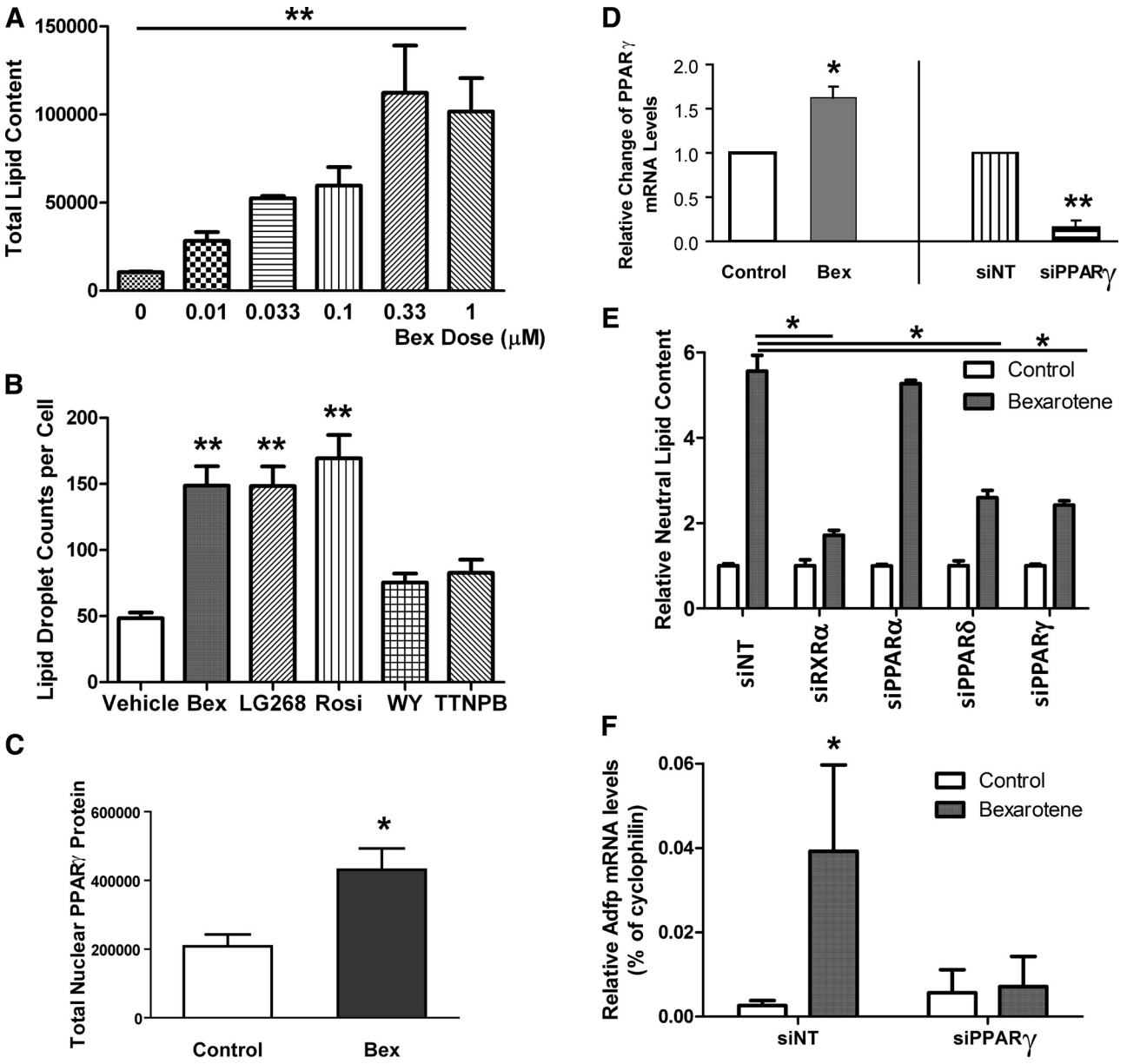

Fig. 3. Characterization of the lipid-accumulative effect of bexarotene on HMECs. A, dose-response relationship of total lipid contents in HMECs treated with bexarotene for 4 days. Lipid contents were measured with high-throughput microscopy (IC-100 system; Beckman Coulter), on the basis of integrated intensity under the lipid masks. B, comparison of lipid droplet counts formed in HMECs in response to agonists of the nuclear receptors RXR [bexarotene (Bex) and LGD100268 (LG268)], PPARγ [rosiglitazone (Rosi)], PPARα [WY14643 (WY)], and RAR [(*E*)-4-[2-(5,6,7,8-tetrahydro-5,5,8,8-tetramethyl-2-naphthalenyl-1-propenyl]benzoic acid (TTNPB)]. C, PPARγ expression levels in cell nuclei after 4 days of bexarotene treatment. PPARγ protein levels were measured with high-throughput microscopy, on the basis of immunofluorescent labeling of the receptor. D, PPARγ mRNA levels after 24 h of treatment with bexarotene (left) and after knockdown with nontargeting control (siNT) or PPARγ-specific (siPPARγ) siRNAs. E, comparison of relative neutral lipid contents in HMECs treated with solvent (control) or bexarotene for 4 days, after knockdown of the nuclear receptors RXRα (siRXRα), PPARα (siPPARα), PPARδ (siPPARδ), or PPARγ (siPPARγ). F, comparison of ADFP mRNA levels in control or bexarotene-treated cells after knockdown with nontargeting control (siNT) or PPARγ-specific (siPPARγ) siRNAs. **, $p < 0.005$; *, $p < 0.05$.

greater degree than its own potency, which resulted in superadditive or synergistic effects (Fig. 5B). The synergistic combinations of rosiglitazone and bexarotene identified by the Calcusyn algorithm included 0.2, 0.66, and 2 μM rosiglitazone and 0.01 to 0.1 μM bexarotene (Fig. 5C). To validate these findings, the effects of combinations were compared with the effects of bexarotene and rosiglitazone applied individually. The combinations that were significantly different from the ED_{50} values of the two individual compounds are shown in Fig. 5D. It is noteworthy that, the various combinations of bexarotene and rosiglitazone were synergistic not across the entire dose range but primarily with low doses (0.01–0.1 μM) of bexarotene and 0.66 to 2 μM doses of rosiglitazone.

The combination of bexarotene and rosiglitazone also resulted in enhanced lipid accumulation, although the interaction between the two agents did not seem to be synergistic with respect to lipid contents. Overall, there was a marked, nonlinear, inverse correlation between cell counts and mean cellular lipid contents after 4 days of treatment when various bexarotene and rosiglitazone combinations were compared ($p < 0.001$) (Fig. 5E). The increase in bexarotene concentra-

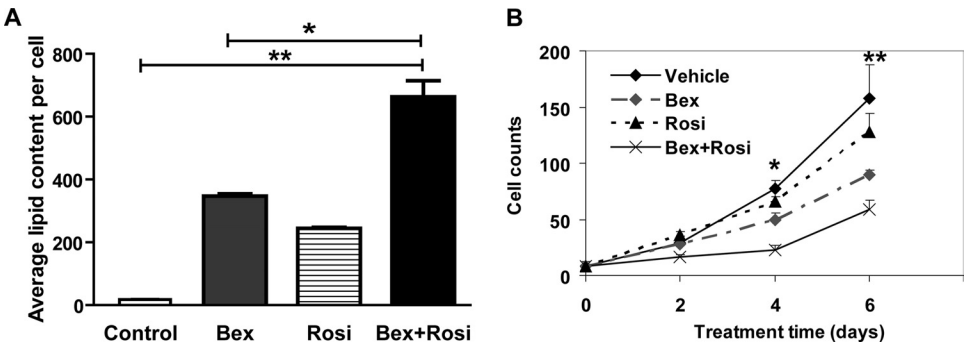

Fig. 4. Lipid-accumulative and growth-suppressive effects of the combination of bexarotene and rosiglitazone in mammary epithelial cells. A, comparison of total neutral lipid contents in HMECs at the end of 6-day treatment with bexarotene (Bex) (1 μM), rosiglitazone (Rosi) (2 μM), or bexarotene and rosiglitazone in combination. B, time-course growth assay comparing cell counts after treatment with bexarotene (1 μM), rosiglitazone (2 μM), or the combination of the two drugs in normal HMECs. **, $p < 0.005$; *, $p < 0.05$.

tion from 0 to 10 nM caused a marked downward shift of the rosiglitazone dose-response curve toward lower cell counts (less proliferation) and a slight shift to the right, which indicated a minimal increase in lipid contents (Fig 5E, arrow a). In contrast, the incremental rosiglitazone doses combined with 100 nM bexarotene resulted in a minor decrease in cell counts but a greater shift to the right (Fig 5E, arrow b), which indicated greater lipid contents. Higher bexarotene doses (e.g., 0.33 and 1 μM) caused further shifts to the right, which indicated even stronger lipid-inducing effects, and less growth suppression. Taken together, the dose pairs of low-dose bexarotene and rosiglitazone with synergistic efficacy for growth suppression did not result in additive lipid accumulation, which indicates that effective growth suppression of mammary epithelial cells can be achieved by using significantly reduced doses of bexarotene combined with rosiglitazone, without proportionate elevations in lipid levels.

Discussion

RXR-selective retinoids such as bexarotene (LGD1069, Targretin) have proved to be very effective agents for the prevention of both ER-positive and ER-negative breast cancers in various animal models and currently are being tested in clinical trials. However, the effective dose of bexarotene is associated with side effects that limit its use as a chemopreventive drug; therefore, the development of dose-reduction strategies has become particularly important. Although the causes of elevated serum triglyceride levels are known, the consequences of rexinoid treatment for lipid metabolism within epithelial cells (the actual target cells for cancer prevention) have not been elucidated. In the present study, we applied a high-content analysis approach to define rexinoid-induced changes in lipid metabolism and cell growth of breast epithelial cells on a cell-by-cell basis, rather than using the usual approach of qualitative assessment of lipid contents in bulk populations. We showed that effective growth suppression of mammary epithelial cells may be achieved by using low doses of bexarotene combined with the PPARγ agonist rosiglitazone, thereby dissociating the adverse systemic effects of bexarotene from the therapeutic antiproliferative effects on the mammary epithelium.

Apart from refractory cutaneous T-cell lymphomas, bexarotene monotherapy failed to demonstrate significant antitumor efficacy or to improve overall survival rates for most cancers; however, combinatorial chemotherapeutic applications of bexarotene seem more promising in several tissues (Khuri et al., 2001; Yen et al., 2004; Dragnev et al., 2005; Cesario et al., 2006). It is noteworthy that rexinoids proved to be highly efficacious chemopreventive agents in a number of preclinical rodent models of breast cancer (Gottardis et al., 1996; Wu et al., 2002; Li et al., 2007). It was noted early on that the antitumor effects correlated with the induction of adipocyte-specific gene expression (Agarwal et al., 2000). However, the effects of rexinoid treatment on lipid metabolism in breast epithelial cells have not been characterized.

The ability to perform quantitative high-content analyses in a multiwell format facilitated acquisition of both singular and combinatorial data using bexarotene and the synthetic PPARγ agonist rosiglitazone. Our data show that bexarotene induces the accumulation of cytoplasmic lipid droplets and this increase in neutral lipid contents is associated with up-regulation of ADFP (adipophilin). In fat and liver cells, the expression of ADFP was shown to correlate directly with fat storage (Brasaemle et al., 1997; Imamura et al., 2002). ADFP is localized at the surface of lipid droplets in adipocytes and a variety of other cells, including fibroblasts, macrophages, hepatocytes, and mammary epithelial cells (Brasaemle et al., 1997), and stimulates lipid accumulation when overexpressed (Imamura et al., 2002). It has been determined that the human ADFP gene is a direct LXR target (Kotokorpi et al., 2010); because an RXR/LXR heterodimer might be activated through the RXR partner, ADFP could potentially be up-regulated by rexinoids. It is noteworthy that knockdown of either LXRα or LXRβ was unable to block lipid droplet formation in HMECs (data not shown), which suggests that the induction of ADFP is not the driving force behind the accumulation of lipid droplets in HMECs. Given the 24-h period needed for the up-regulation of ADFP, bexarotene may not have a direct transcriptional effect on the ADFP gene itself. Nevertheless, the association of the lipid droplets with ADFP raises the possibility that the metabolic changes observed in response to bexarotene are associated with the activation of differentiation processes.

Although the suppression of RXRα through RNA interference indicated that RXRα was required for activation of the lipogenic pathway, no correlation between RXR expression levels and lipid accumulation was observed through examination on a cell-by-cell basis, at the time the biochemical changes were observed. It should be noted, however, that the functional impact of receptor levels and localization on accumulation of lipid droplets cannot be readily studied in the same experiment, because of the different time frames of the two processes. Lipid droplet formation as a biochemical consequence follows receptor activation by several days. Given the abundant levels of RXRα in mammary epithelial cells, the data also suggest that it may not be a limiting factor in the signaling pathway and/or it has little or no regulation

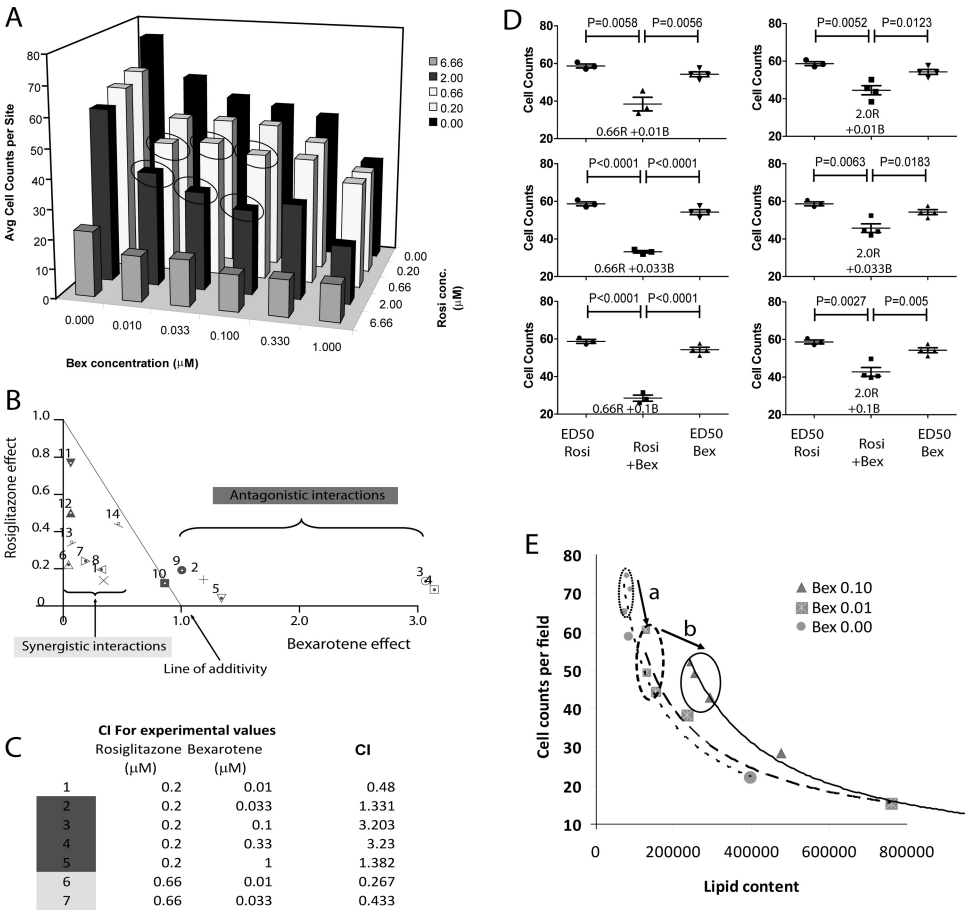

Fig. 5. Synergistic growth-suppressive effects on HMECs of combined doses of bexarotene and rosiglitazone. A, high-throughput microscopy was used to compare cell counts after 4 days of treatment with bexarotene (Bex), rosiglitazone (Rosi), or the two drugs in combination. Means of average cell counts from triplicate wells with 45 imaged microscopic fields per well are shown for each drug concentration. The data bars corresponding to the six bexarotene/rosiglitazone combinations confirmed in D as statistically significantly different, compared with the ED_{50} values of the two individual compounds, and thus synergistic are circled. B, isobologram analysis comparing the effects of bexarotene/rosiglitazone dose pairs on the basis of dose-effect calculations obtained through the median effects method (Chou and Talalay, 1984). Dose values of single agents with equal potencies mark the line of additivity, which segregates dose pairs with synergistic and antagonistic interactions between two dugs. C, table summarizing doses of bexarotene and rosiglitazone and the combination indexes derived from the resulting isobologram (only combinations containing 0.2, 0.66, and 2 μM rosiglitazone are shown). Combination index (CI) values of less than 0.9 indicate synergy, whereas values of more than 1.3 indicate antagonism. The identification numbers for combinations found to be synergistic or antagonistic in the secondary tests (see D) are highlighted with a light gray background, and those found to be antagonistic are highlighted with a dark gray background. D, statistical evaluation of synergism. The significance of the synergistic effect associated with dual bexarotene/rosiglitazone treatment was established through direct comparison, with two-tailed Student's *t* tests, of variant dose combinations with the relative effects of the two individual drugs at ED_{50}, as described previously by Laska et al. (1994). E, scatter plots of cell growth and lipid accumulation of HMECs treated with 0, 10, or 100 nM bexarotene in conjunction with increasing doses of rosiglitazone (0, 0.2, 0.66, 2, and 6.66 μM, represented by data points of proportionally increasing size within each of the three bexarotene treatment groups). The directional shifts of the dose-response curves are indicated by arrows a and b. Each data point represents the mean of four replicate wells, and values are plotted according to average cellular lipid contents and cell counts per field (as shown on *y*-axis of E).

during lipid accumulation. PPARs are intricately involved in the regulation of lipid metabolism and preadipocyte differentiation (Hartig et al., 2011). A report on a genome-wide search for direct targets for RXR/PPARγ binding sites during adipogenesis showed that such sites are predominantly present in the class of genes involved in lipid and steroid metabolism (Hamza et al., 2009). Although PPARγ activity enables ErbB2-positive breast cancer cells (which produce high levels of fat) to convert fatty acids to triglycerides and thereby to evade lipid-induced apoptosis (Kourtidis et al., 2009), other studies suggested that PPARγ is involved in regulating the growth and differentiation of a number of different cancer cells (Rosen and Spiegelman, 2001; Michalik et al., 2004). The ability of rosiglitazone to prevent hyperplasia indicated its potential use as a chemopreventive agent (Sporn et al., 2001; Wu et al., 2008). Our data showed that, in nonmalignant breast epithelial cells, bexarotene, while suppressing cell growth, also activated a PPARγ-mediated pathway responsible for the conversion of fatty acids to triglycerides. This feed-forward mechanism resulting in the induction of PPARγ might partially explain the synergistic relationship between bexarotene and rosiglitazone. Conversely, the elevated cellular lipid contents produced in response to various concentrations of bexarotene showed a strict inverse correla-

tion with the proliferative ability of primary mammary cells. Therefore, the neutral lipid content should be considered and studied as a novel diagnostic or potentially predictive marker of chemopreventive activity. Similar to chemotherapy, combination treatment to achieve cancer prevention has been proposed; promising preclinical studies have demonstrated the potential therapeutic benefits associated with rexinoids administered in combination with drugs that act through alternative mechanisms (Sporn, 1980; Liby et al., 2006; Brown et al., 2008). Some early studies indicated the potential chemopreventive effects that combined retinoid and troglitazone treatment might have on chemically induced, preneoplastic lesion formation (Mehta et al., 2000). However, it is the concept of using a markedly reduced dose of the highly effective chemopreventive agent bexarotene in combination with a synergistic drug that should warrant long-term treatment of patients for cancer-preventive purposes. An in vivo study is needed to validate the feasibility of this concept.

Rosiglitazone was shown to potentiate the effect of bexarotene in suppressing the proliferation and accumulation of neutral lipids; moreover, combined treatment synergistically inhibited cell proliferation at bexarotene doses markedly lower than its IC_{50}. Clinical treatment regimens of bexarotene in the range of 100 to 400 mg/m^2 doses per day may result in serum drug levels exceeding 1 μM (Miller et al., 1997; Rizvi et al., 1999). This dosage alone may cause mild to severe hyperlipidemia in more than 80% of the patients, necessitating dose reduction or lipid-lowering treatment (Assaf et al., 2006). We show that bexarotene concentrations as low as 10 nM effectively inhibit cell proliferation in vitro when combined with rosiglitazone. It is noteworthy that although the addition of rosiglitazone to bexarotene sensitizes breast epithelial cells to the antiproliferative effect of bexarotene, it seems to blunt the cells' sensitivity to the induction of lipid accumulation. This implies that the genes involved in mediating growth suppression are regulated differently by the combination of low-dose bexarotene and rosiglitazone, compared with the genes required for triglyceride synthesis. This observation may provide the basis for combination treatment with low-dose (10–100 nM) bexarotene and other agents similarly synergistic with bexarotene with respect to growth suppression but either nonadditive or antagonistic with respect to lipid accumulation.

Despite controversy regarding the clinical safety of rosiglitazone, thiazolidinediones remain important in the treatment of type 2 diabetes, pending careful assessment of cardiovascular risks (Kahn and McGraw, 2010; Schernthaner and Chilton, 2010). On the basis of this report as a proof-of-concept study, other agonists and small-molecule compounds that activate PPARγ should be evaluated for their ability to suppress cell growth, to inhibit transformation, or to prevent breast cancer in animal models when used in combination with a rexinoid.

Acknowledgments

We acknowledge Dr. Michelle Savage and Dr. Zoltan Balajthy for critical reading of the manuscript.

Authorship Contributions

Participated in research design: Uray, Brown, and Mancini.
Conducted experiments: Uray and Rodenberg.
Contributed new reagents or analytic tools: Uray, Bissonnette, Brown, and Mancini.
Performed data analysis: Uray.
Wrote or contributed to the writing of the manuscript: Uray and Mancini.

References

Abba MC, Hu Y, Levy CC, Gaddis S, Kittrell FS, Zhang Y, Hill J, Bissonnette RP, Medina D, Brown PH, et al. (2008) Transcriptomic signature of bexarotene (rexinoid LGD1069) on mammary gland from three transgenic mouse mammary cancer models. *BMC Med Genomics* **1:**40.
Agarwal VR, Bischoff ED, Hermann T, and Lamph WW (2000) Induction of adipocyte-specific gene expression is correlated with mammary tumor regression by the retinoid X receptor-ligand LGD1069 (targretin). *Cancer Res* **60:**6033–6038.
Assaf C, Bagot M, Dummer R, Duvic M, Gniadecki R, Knobler R, Ranki A, Schwandt P, and Whittaker S (2006) Minimizing adverse side-effects of oral bexarotene in cutaneous T-cell lymphoma: an expert opinion. *Br J Dermatol* **155:**261–266.
Bischoff ED, Heyman RA, and Lamph WW (1999) Effect of the retinoid X receptor-selective ligand LGD1069 on mammary carcinoma after tamoxifen failure. *J Natl Cancer Inst* **91:**2118.
Blumenschein GR Jr, Khuri FR, von Pawel J, Gatzemeier U, Miller WH Jr, Jotte RM, Le Treut J, Sun SL, Zhang JK, Dziewanowska ZE, et al. (2008) Phase III trial comparing carboplatin, paclitaxel, and bexarotene with carboplatin and paclitaxel in chemotherapy-naive patients with advanced or metastatic non-small-cell lung cancer: SPIRIT II. *J Clin Oncol* **26:**1879–1885.
Brasaemle DL, Barber T, Wolins NE, Serrero G, Blanchette-Mackie EJ, and Londos C (1997) Adipose differentiation-related protein is an ubiquitously expressed lipid storage droplet-associated protein. *J Lipid Res* **38:**2249–2263.
Brown PH, Subbaramaiah K, Salmon AP, Baker R, Newman RA, Yang P, Zhou XK, Bissonnette RP, Dannenberg AJ, and Howe LR (2008) Combination chemoprevention of HER2/neu-induced breast cancer using a cyclooxygenase-2 inhibitor and a retinoid X receptor-selective retinoid. *Cancer Prev Res (Phila)* **1:**208–214.
Cesario RM, Stone J, Yen WC, Bissonnette RP, and Lamph WW (2006) Differentiation and growth inhibition mediated via the RXR:PPARgamma heterodimer in colon cancer. *Cancer Lett* **240:**225–233.
Chou TC and Talalay P (1984) Quantitative analysis of dose-effect relationships: the combined effects of multiple drugs or enzyme inhibitors. *Adv Enzyme Regul* **22:**27–55.
Cuzick J, Powles T, Veronesi U, Forbes J, Edwards R, Ashley S, and Boyle P (2003) Overview of the main outcomes in breast-cancer prevention trials. *Lancet* **361:**296–300.
de Vries-van der Weij J, de Haan W, Hu L, Kuif M, Oei HL, van der Hoorn JW, Havekes LM, Princen HM, Romijn JA, Smit JW, et al. (2009) Bexarotene induces dyslipidemia by increased very low-density lipoprotein production and cholesteryl ester transfer protein-mediated reduction of high-density lipoprotein. *Endocrinology* **150:**2368–2375.
Dragnev KH, Petty WJ, Ma Y, Rigas JR, and Dmitrovsky E (2005) Nonclassical retinoids and lung carcinogenesis. *Clin Lung Cancer* **6:**237–244.
Gottardis MM, Bischoff ED, Shirley MA, Wagoner MA, Lamph WW, and Heyman RA (1996) Chemoprevention of mammary carcinoma by LGD1069 (Targretin): an RXR-selective ligand. *Cancer Res* **56:**5566–5570.
Hamza MS, Pott S, Vega VB, Thomsen JS, Kandhadayar GS, Ng PW, Chiu KP, Pettersson S, Wei CL, Ruan Y, et al. (2009) De-novo identification of PPARgamma/RXR binding sites and direct targets during adipogenesis. *PLoS One* **4:**e4907.
Hartig SM, He B, Long W, Buehrer BM, and Mancini MA (2011) Homeostatic levels of SRC-2 and SRC-3 promote early human adipogenesis. *J Cell Biol* **192:**55–67.
Imamura M, Inoguchi T, Ikuyama S, Taniguchi S, Kobayashi K, Nakashima N, and Nawata H (2002) ADRP stimulates lipid accumulation and lipid droplet formation in murine fibroblasts. *Am J Physiol Endocrinol Metab* **283:**E775–E783.
Kahn BB and McGraw TE (2010) Rosiglitazone, PPARγ, and type 2 diabetes. *N Engl J Med* **363:**2667–2669.
Khuri FR, Rigas JR, Figlin RA, Gralla RJ, Shin DM, Munden R, Fox N, Huyghe MR, Kean Y, Reich SD, et al. (2001) Multi-institutional phase I/II trial of oral bexarotene in combination with cisplatin and vinorelbine in previously untreated patients with advanced non-small-cell lung cancer. *J Clin Oncol* **19:**2626–2637.
Kim HT, Kong G, Denardo D, Li Y, Uray I, Pal S, Mohsin S, Hilsenbeck SG, Bissonnette R, Lamph WW, et al. (2006) Identification of biomarkers modulated by the rexinoid LGD1069 (bexarotene) in human breast cells using oligonucleotide arrays. *Cancer Res* **66:**12009–12018.
Kotokorpi P, Venteclef N, Ellis E, Gustafsson JA, and Mode A (2010) The human ADFP gene is a direct liver-X-receptor (LXR) target gene and differentially regulated by synthetic LXR ligands. *Mol Pharmacol* **77:**79–86.
Kourtidis A, Srinivasaiah R, Carkner RD, Brosnan MJ, and Conklin DS (2009) Peroxisome proliferator-activated receptor-gamma protects ERBB2-positive breast cancer cells from palmitate toxicity. *Breast Cancer Res* **11:**R16.
Laska EM, Meisner M, and Siegel C (1994) Simple designs and model-free tests for synergy. *Biometrics* **50:**834–841.
Li Y, Zhang Y, Hill J, Shen Q, Kim HT, Xu X, Hilsenbeck SG, Bissonnette RP, Lamph WW, and Brown PH (2007) The rexinoid LG100268 prevents the development of preinvasive and invasive estrogen receptor negative tumors in MMTV-erbB2 mice. *Clin Cancer Res* **13:**6224–6231.
Liby K, Rendi M, Suh N, Royce DB, Risingsong R, Williams CR, Lamph W, Labrie F, Krajewski S, Xu X, et al. (2006) The combination of the rexinoid, LG100268, and a selective estrogen receptor modulator, either arzoxifene or acolbifene, synergizes in the prevention and treatment of mammary tumors in an estrogen receptor-negative model of breast cancer. *Clin Cancer Res* **12:**5902–5909.
McDonough PM, Agustin RM, Ingermanson RS, Loy PA, Buehrer BM, Nicoll JB, Prigozhina NL, Mikic I, and Price JH (2009) Quantification of lipid droplets and

associated proteins in cellular models of obesity via high-content/high-throughput microscopy and automated image analysis. *Assay Drug Dev Technol* **7:**440–460.
Mehta RG, Williamson E, Patel MK, and Koeffler HP (2000) A ligand of peroxisome proliferator-activated receptor gamma, retinoids, and prevention of preneoplastic mammary lesions. *J Natl Cancer Inst* **92:**418–423.
Michalik L, Desvergne B, and Wahli W (2004) Peroxisome-proliferator-activated receptors and cancers: complex stories. *Nat Rev Cancer* **4:**61–70.
Miller VA, Benedetti FM, Rigas JR, Verret AL, Pfister DG, Straus D, Kris MG, Crisp M, Heyman R, Loewen GR, et al. (1997) Initial clinical trial of a selective retinoid X receptor ligand, LGD1069. *J Clin Oncol* **15:**790–795.
Rizvi NA, Marshall JL, Dahut W, Ness E, Truglia JA, Loewen G, Gill GM, Ulm EH, Geiser R, Jaunakais D, et al. (1999) A phase I study of LGD1069 in adults with advanced cancer. *Clin Cancer Res* **5:**1658–1664.
Rosen ED and Spiegelman BM (2001) PPARgamma: a nuclear regulator of metabolism, differentiation, and cell growth. *J Biol Chem* **276:**37731–37734.
Russell TD, Palmer CA, Orlicky DJ, Fischer A, Rudolph MC, Neville MC, and McManaman JL (2007) Cytoplasmic lipid droplet accumulation in developing mammary epithelial cells: roles of adipophilin and lipid metabolism. *J Lipid Res* **48:**1463–1475.
Schernthaner G and Chilton RJ (2010) Cardiovascular risk and thiazolidinediones: what do meta-analyses really tell us? *Diabetes Obes Metab* **12:**1023–1035.
Sporn MB (1980) Combination chemoprevention of cancer. *Nature* **287:**107–108.
Sporn MB, Suh N, and Mangelsdorf DJ (2001) Prospects for prevention and treatment of cancer with selective PPARgamma modulators (SPARMs). *Trends Mol Med* **7:**395–400.
Uray IP and Brown PH (2006) Prevention of breast cancer: current state of the science and future opportunities. *Expert Opin Investig Drugs* **15:**1583–1600.
Uray IP and Brown PH (2011) Chemoprevention of hormone receptor-negative breast cancer: new approaches needed. *Recent Results Cancer Res* **188:**147–162.
Uray IP, Shen Q, Seo HS, Kim H, Lamph WW, Bissonnette RP, and Brown PH (2009) Rexinoid-induced expression of IGFBP-6 requires RARbeta-dependent permissive cooperation of retinoid receptors and AP-1. *J Biol Chem* **284:**345–353.
Wu K, DuPré E, Kim H, Tin-U CK, Bissonnette RP, Lamph WW, and Brown PH (2006) Receptor-selective retinoids inhibit the growth of normal and malignant breast cells by inducing G_1 cell cycle blockade. *Breast Cancer Res Treat* **96:**147–157.
Wu K, Kim HT, Rodriquez JL, Hilsenbeck SG, Mohsin SK, Xu XC, Lamph WW, Kuhn JG, Green JE, and Brown PH (2002) Suppression of mammary tumorigenesis in transgenic mice by the RXR-selective retinoid, LGD1069. *Cancer Epidemiol Biomarkers Prev* **11:**467–474.
Wu W, Celestino J, Milam MR, Schmeler KM, Broaddus RR, Ellenson LH, and Lu KH (2008) Primary chemoprevention of endometrial hyperplasia with the peroxisome proliferator-activated receptor gamma agonist rosiglitazone in the PTEN heterozygote murine model. *Int J Gynecol Cancer* **18:**329–338.
Yen WC, Prudente RY, and Lamph WW (2004) Synergistic effect of a retinoid X receptor-selective ligand bexarotene (LGD1069, Targretin) and paclitaxel (Taxol) in mammary carcinoma. *Breast Cancer Res Treat* **88:**141–148.
Zhang JH, Chung TD, and Oldenburg KR (1999) A simple statistical parameter for use in evaluation and validation of high throughput screening assays. *J Biomol Screen* **4:**67–73.

Address correspondence to: Dr. M. A. Mancini, Department of Molecular and Cellular Biology, Baylor College of Medicine, One Baylor Plaza, MS 600, Houston, TX 77030. E-mail: mancini@bcm.tmc.edu